Microchim Acta (2017) 184:533–540
DOI 10.1007/s00604-016-2047-5

ORIGINAL PAPER

Voltammetric determination of nonylphenol using a glassy carbon electrode modified with a nanocomposite consisting of CTAB, Fe_3O_4 nanoparticles and reduced graphene oxide

Jing Zou[1] · Manli Guo[1] · Yanlong Feng[1] · Mei Yang[1] · Yujuan Cao[1] · Debin Zhu[1] · Ying Yu[1]

Received: 27 July 2016 / Accepted: 5 December 2016 / Published online: 10 December 2016

Abstract A nanocomposite consisting of cetyltrimethylammonium bromide (CTAB), Fe_3O_4 nanoparticles and reduced graphene oxide (CTAB-Fe_3O_4-rGO) was prepared, characterized, and used to modify the surface of a glassy carbon electrode (GCE). The voltammetric response of the modified GCE to 4-nonylphenol (NPh) was investigated by cyclic voltammetry and revealed a strong peak at around 0.57 V (vs. SCE). Under optimum conditions, the calibration plot is linear in the ranges from 0.03 to 7.0 μM and from 7.0 to 15.0 μM, with a 8 nM detection limit which is lower that that of many other methods. The modified electrode has excellent fabrication reproducibility and was applied to the determination of NPh in spiked real water samples to give recoveries (at a spiking level of 1 μM) between 102.1 and 99.1%.

Keywords Nanocomposite · Electroanalysis · Nonylphenol · Differential pulse voltammetry · Graphene oxide · Endocrine disrupting chemical · Water analysis · Cationic detergent · Magnetic nanoparticles

Electronic supplementary material The online version of this article (doi:10.1007/s00604-016-2047-5) contains supplementary material, which is available to authorized users.

✉ Manli Guo
manliguo@163.com

[1] Key Laboratory of Analytical Chemistry for Biomedicine (Guangzhou), School of Chemistry and Environment, South China Normal University, Guangzhou 510006, People's Republic of China

Introduction

Nonylphenol ethoxylates (NPEs), a major class of nonionic surfactants, are widely used in industrial, institutional, commercial and household applications such as detergents, wetting and dispersing agents [1]. Nonylphenol (NPh), the major degradation product of NPEs, is persistent in the aquatic environment, moderately bioaccumulative and more toxic to aquatic life than its precursors [2]. Nowadays, NPh is known as one of the Endocrine Disrupting Chemicals (EDCs) and is identified as a ubiquitous pollutant in urban aquatic environments, with concentrations on the order of parts per billion [3]. Because of its high hydrophobicity, low degradation rate, stability and endocrine disrupting activity, NPh has been designated as a priority hazardous substance (PHS) in the Water Framework Directive and most of its use are currently regulated [4]. Thus, it is necessary to develop efficient methods for NPh monitoring.

At present, various methods have been developed for the detection and quantification of NPh, such as gas chromatography/mass spectrometry (GC/MS) [5], liquid chromatography/mass spectrometry (LC/MS) [6, 7], high-performance liquid chromatography (HPLC) [8, 9], molecularly imprinted technique [10, 11], and enzyme linked immunosorbent assay (ELISA) [12]. Many of these detection methods are sensitive but some of them are expensive, need tedious procedures and need skilled operators. Compared with them, electrochemical techniques possess the advantages of rapid response, low cost, high sensitivity, and real-time monitoring ability. In order to enhance the electrochemical response of NPh, different modified electrodes have been developed based on various nanocomposites. For example, Zhang et al. developed a molecularly imprinted electrochemical sensor based on sol-gel technology and multiwalled carbon nanotubes (MWNTs)-Nafion

functional layer for 2-nonylphenol detection and a detection limit of 0.06 μM was obtained [11].

Graphene, a two-dimensional (2D) single-atomic-layer carbon material, has attracted enormous attention in constructing electrochemical sensors because of its large surface area, excellent electrical conductivity, high electro-catalytic activity and thermal stability [13–15]. Several kinds of graphene-based nanocomposites modified electrodes, such as the reduced graphene-DNA hybrid modified glassy carbon electrode (GCE) [16], the thiol-β-cyclodextrin and graphene modified gold electrode [17], and the graphene-chitosan modified GCE [18] have been fabricated for the sensitive electrochemical detection of NPh. Magnetic Fe_3O_4 nanoparticles possess unusual structural, excellent adsorption, catalytic properties and inherent electrical conductivity. Fe_3O_4/graphene hybrid materials formed through the combination of Fe_3O_4 nanoparticles with graphene have been utilized for the construction of sensitive electrochemical sensing platforms [19–22]. Cetyltrimethylammonium bromide (CTAB), a cationic surfactant which has a hydrophilic head on one side and a long hydrophobic tail on the other side, has been extensively employed to enhance sensitivity of electrochemical sensors because of the high accumulation efficiency of CTAB toward target molecules through electrostatic interaction or hydrophobic interaction [23–26]. A remarkable enhancement of the electrochemical oxidation of NPh has been achieved by using a CTAB modified carbon paste electrode [27].

CTAB functionalized magnetic Fe_3O_4-reduced graphene oxide ternary nanocomposite (CTAB-Fe_3O_4-rGO) was prepared and used for the modification of glassy carbon electrode for the electrochemical determination of NPh. The electrochemical behavior of NPh at the modified electrode was investigated by cyclic voltammetry, and the factors influencing the differential pulse voltammetric (DPV) response of NPh were optimized. The modified electrode was also applied to determine NPh in real water samples.

Experimental

Materials

Graphene oxide powder (GO) and monolayer graphene powder (GR) were purchased from Nanjing XFNANO Materials Tech Co., Ltd. (Nanjing, China, www.xfnano.com). Ammonia ($NH_3 \cdot H_2O$), cetyltrimethylammonium bromide (CTAB), ferrous chloride tetrahydrate ($FeCl_2 \cdot 4H_2O$), sodium dodecyl sulfate (SDS), Tween-80 and N,N-dimethylformamide (DMF) were obtained from Guangzhou Chemical Reagent Factory (Guangzhou, China, www.chemicalreagent.com). 4-Nonylphenol (NPh, guaranteed reagent) was purchased from Macklin Biochemical Co., Ltd. (Shanghai, China, www.macklin.cn), and its stock solution (0.01 M) was prepared with ethanol. Phosphate buffer (0.1 M) was prepared with Na_2HPO_4 and KH_2PO_4, and the pH value of each solution was adjusted with HCl or NaOH solution by using a PHSJ-3F pH-meter. All other chemicals were of analytical grade. Ultrapure water was used throughout the experiments.

Preparation of CTAB-Fe_3O_4-rGO nanocomposite

The CTAB-Fe_3O_4-rGO nanocomposite was prepared via the redox reaction between GO and Fe^{2+} based on the report by Xue et al. [28] with some modifications. First, GO was dispersed in water under sonication to form a brown solution. CTAB (mass ratio of CTAB to GO =10:1) was added to GO solution (0.2 mg mL^{-1}) under ultrasonic agitation for 2 h. The CTAB-GO suspension was let stand for 1 h. Next, $FeCl_2 \cdot 4H_2O$ (mass ratio of $FeCl_2 \cdot 4H_2O$ to GO =20:1) was dissolved in the CTAB-GO solution. Then, $NH_3 \cdot H_2O$ was slowly added into the mixed suspension until the pH value of the solution reached 10. The black nanocomposite was separated with a magnet, washed with ethanol and water for several times, respectively, and finally dried in vacuum at 50 °C (Scheme 1). For comparison, Tween-80-Fe_3O_4-rGO and SDS-Fe_3O_4-rGO nanocomposites were prepared, and Fe_3O_4-rGO nanocomposite was also prepared according to the above procedures without the addition of CTAB.

Preparation of modified electrodes

A glassy carbon electrode (GCE, 2 mm in diameter, purchased from TianJin AIDAhengsheng Science-Technology Development Co., Ltd., Tianjin China, www.tjaida.cn) was polished to a mirror-like surface with 0.05 μm alumina slurry, sequentially cleaned by sonicating in ethanol and water, and then dried in a stream of high-purity nitrogen. Prior to use, the prepared CTAB-Fe_3O_4-rGO nanocomposite was dispersed in water with a final concentration of 1 mg mL^{-1} under sonication for 30 min. Then, 4 μL of the suspension was cast onto a GCE surface and dried under an infrared lamp, and thus the CTAB-Fe_3O_4-rGO modified GCE (CTAB-Fe_3O_4-rGO/GCE) was prepared. In control experiments, CTAB modified GCE (CTAB/GCE) and Fe_3O_4-rGO modified GCE (Fe_3O_4-rGO/GCE) were prepared by casting 1 mg mL^{-1} CTAB aqueous solution and 1 mg mL^{-1} Fe_3O_4-rGO suspension, respectively, onto GCE surfaces. GR modified GCE (GR/GCE) was

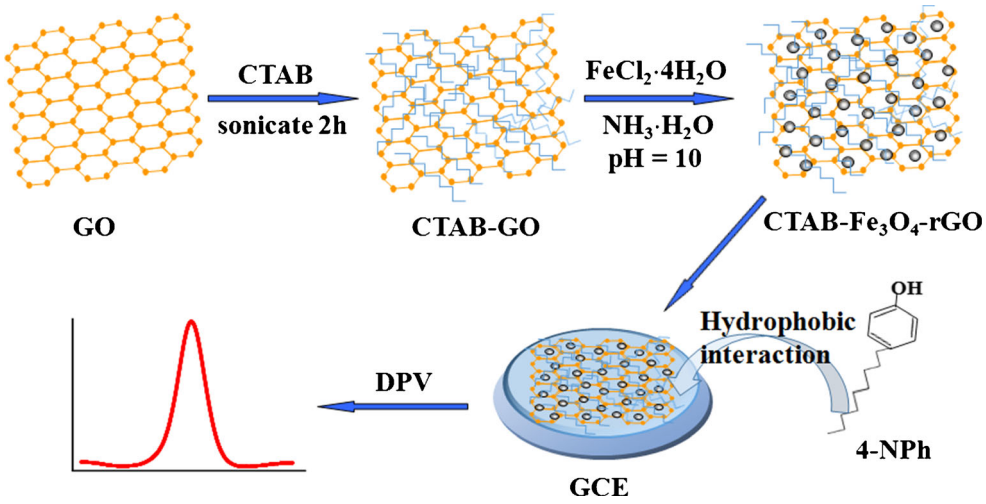

Scheme 1 Illustration of the preparation procedure of CTAB-Fe_3O_4-rGO nanocomposite and the process of electrochemical detection

also prepared by casting the dispersion of GR in DMF (1 mg mL^{-1}) onto a GCE surface.

Characterizations and electrochemical measurements

The morphology of CTAB-Fe_3O_4-rGO was characterized with a FEI Tecnai G20 transmission electron microscope (TEM). X-ray diffraction (XRD) analysis was recorded on a Bruker D8 Advance X-ray diffractometer implementing with Cu-Kα radiation (λ = 1.5418 Å). X-ray photoelectron spectroscopy (XPS) measurement was performed with a Escalab 250XI spectrometer (Thermo Fisher Scientific) equipped with an Al Kα monochromatic X-ray source.

Cyclic voltammetry (CV) and differential pulse voltammetry (DPV) were carried out with a CHI660E electrochemical workstation (Chenhua, Shanghai, China, www.chinstr.com). A GCE or a modified GCE was used as the working electrode. The reference electrode was a saturated calomel electrode (SCE), and a platinum wire worked as the counter electrode.

Cyclic voltammetry of different electrodes were recorded in the potential range of −0.2 and 0.6 V in 5 mM $K_3Fe(CN)_6$/$K_4Fe(CN)_6$ (1:1) aqueous solution containing 0.1 M KCl as the supporting electrolyte at a scan rate of 0.05 V s^{-1}. The electrochemical oxidation of NPh was investigated by CV and DPV. Before each measurement, the electrode was treated by potential cycling between 0.2 and 0.9 V in 0.1 M phosphate buffer until a stable cyclic voltammogram was obtained. The accumulation of NPh on an electrode surface was performed at −0.1 V for 300 s, then CV and DPV curves were recorded in the potential range of 0.2 and 0.9 V. All electrochemical measurements were performed at room temperature.

For determining the NPh contents in real samples, the water samples collected from Yan Lake (on our campus) and Pearl River (China) were first filtrated. Desired amounts of Na_2HPO_4 and KH_2PO_4 were added in the filtrate, and the pH value was adjusted to be 7.0. The NPh contents in water samples were measured by DPV before and after the addition of 1 μM NPh. Each sample was measured three times.

Results and discussion

Choice of materials

A nanocomposite consisting of CTAB, Fe_3O_4 nanoparticles and reduced graphene oxide (CTAB-Fe_3O_4-rGO) was designed as an electrode material for the electrochemical determination of NPh. The solution processability of GO facilitates functionalization of graphene nanosheets. A cationic detergent CTAB can interact with GO through electrostatic interaction. Fe_3O_4 nanoparticles were deposited onto the self-reduced GO (rGO) sheets based on the redox reaction between GO and Fe^{2+} [28]. It is expected that the electrochemical oxidation current of NPh at the CTAB-Fe_3O_4-rGO modified electrode can be significantly increased due to the accumulation of NPh at the electrode surface through the hydrophobic interaction with CTAB, the large surface area and good electrical conductivity of Fe_3O_4-rGO.

Characterization of the CTAB-Fe_3O_4-rGO nanocomposite

The morphology of our prepared nanocomposite was characterized by TEM. As shown in Fig. 1, the wrinkled flake-like shape of graphene can be clearly observed, and the 2D nanosheets are well decorated by lots of spherical nanoparticles with an average size of about 22 nm. In the XRD pattern (Fig. S1A), the main peaks at 30.3°, 35.7°, 43.4°, 53.3°, 57.3° and 62.9° marked by their indices (220), (311), (400), (422), (511) and (440), respectively, display the typical characteristics of cubic Fe_3O_4 with a face-centered cubic structure [29]. The presence of N1 s peak in the XPS spectra (Fig. S1B

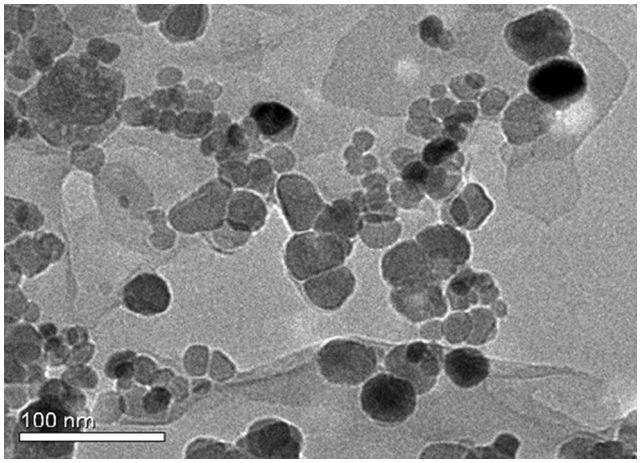

Fig. 1 TEM image of the CTAB-Fe_3O_4-rGO nanocomposite

and Fig. S1C) corresponding to the amine structure in CTAB indicates the existence of CTAB in the prepared nanocomposite. These results indicate that CTAB-Fe_3O_4-rGO nanocomposite has been successfully prepared.

The electrical conductivity of the CTAB-Fe_3O_4-rGO/GCE was measured by CV using $Fe(CN)_6^{3-/4-}$ as a redox probe. As shown in Fig. 2, compared with bare GCE (curve a) and Fe_3O_4-rGO/GCE (curve b), the CTAB-Fe_3O_4-rGO/GCE exhibits the largest redox peak currents and the smallest peak-to-peak separation (curve c). The effective surface area of each electrode was calculated by using the Randles-Sevcik Eq. [30] (at 25 °C): $I_p = 2.69 \times 10^5\ AD^{1/2}n^{3/2}v^{1/2}C$ s, where I_p is the peak current (A); A is the effective surface area of electrode (cm^2); D is the diffusion coefficient, which is 6.3×10^{-6} cm^2 s^{-1} for $Fe(CN)_6^{3-/4-}$ in 0.1 M KCl; n means the number of electrons transferred in the redox reaction, which is 1 for $Fe(CN)_6^{3-/4-}$; v means the scan rate (V s^{-1}); and C is the $Fe(CN)_6^{3-/4-}$ concentration (mol cm^{-3}). The results present the trend of bare GCE (0.0291 cm^2) < Fe_3O_4-rGO/GCE (0.0313 cm^2) < CTAB-Fe_3O_4-rGO/GCE (0.0323 cm^2). This indicates that the prepared CTAB-Fe_3O_4-rGO nanocomposite exhibit large surface area, which makes them beneficial for use as electrode materials.

Voltammetric behaviors of NPh at the CTAB-Fe_3O_4-rGO/GCE

Figure 3 shows the voltammetric behaviors of NPh at bare GCE, CTAB/GCE, Fe_3O_4-rGO/GCE and CTAB-Fe_3O_4-rGO/GCE. Only one anodic peak and no reduction peak can be observed, suggesting that the electrochemical oxidation of NPh is totally irreversible. Compared with bare GCE, the CTAB/GCE exhibits two times larger oxidation peak current (I_p), indicating the accumulation ability of CTAB toward NPh. The oxidation peak potential (E_p) at the CTAB/GCE (0.583 V) is more positive than that at the bare GCE (0.522 V), which is probably due to the poor electrical conductivity of CTAB. The I_p at the CTAB-Fe_3O_4-rGO/GCE is about 4.7 and 1.8 times larger than that at bare GCE and Fe_3O_4-rGO/GCE, respectively. The remarkable increase of I_p value at the CTAB-Fe_3O_4-rGO/GCE might be attributed to the synergistic effect between Fe_3O_4-rGO and CTAB. CTAB with a long alkyl chain accumulates NPh via hydrophobic interactions [27], and the rGO sheets decorated with Fe_3O_4 nanoparticles with a large specific surface area exhibit electrocatalytic activity to the oxidation of NPh.

For comparison, the oxidation of NPh at graphene modified GCE (GR/GCE) was also studied. It has been found that the GR/GCE exhibits a slightly smaller I_p value, while the background current is about 5.4 times larger than that at the CTAB-Fe_3O_4-rGO/GCE (Fig. S2), which is not beneficial in electrochemical sensing application. A neutral detergent (Tween-80) and an anionic detergent (SDS) were also used to prepare Tween-80-Fe_3O_4-rGO and SDS-Fe_3O_4-rGO

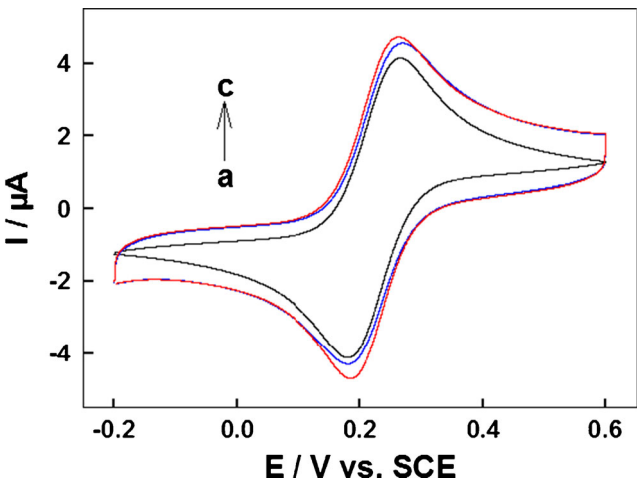

Fig. 2 Cyclic voltammograms of (**a**) bare GCE, (**b**) Fe_3O_4-rGO/GCE, and (**c**) CTAB-Fe_3O_4-rGO/GCE in 5.0 mM $K_3Fe(CN)_6$ + 5.0 mM $K_4Fe(CN)_6$ solution containing 0.1 M KCl. Scan rate: 0.05 V s^{-1}

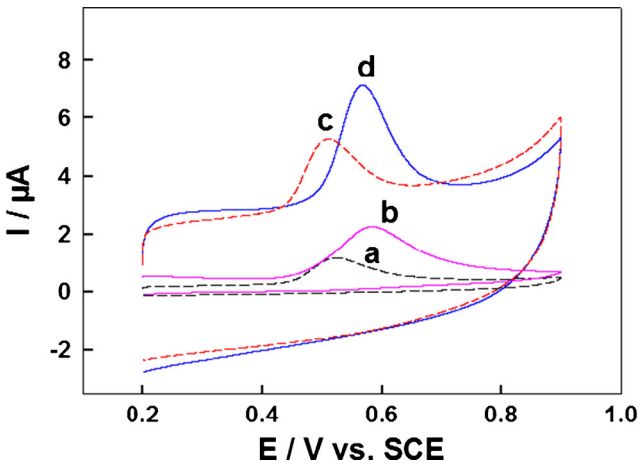

Fig. 3 Cyclic voltammograms of (**a**) bare GCE, (**b**) CTAB/GCE, (**c**) Fe_3O_4-rGO/GCE, and (**d**) CTAB-Fe_3O_4-rGO/GCE in 0.1 M phosphate buffer (pH = 7.0) containing 3 μM NPh. Accumulation potential: −0.1 V; accumulation time: 300 s; scan rate: 0.05 V s^{-1}

nanocomposites for the detection of NPh. The CTAB-Fe_3O_4-rGO/GCE gives the largest response current (Fig. S3), which is probably due to the effective electrostatic interaction between the cationic detergent CTAB with the negatively charged GO. Therefore, the CTAB-Fe_3O_4-rGO/GCE fabricated in our work exhibits a great potential for application in the sensitive electrochemical detection of NPh.

To effect of scan rate (ν) on the voltammetric behavior of NPh at the CTAB-Fe_3O_4-rGO/GCE was investigated. The oxidation peak currents of NPh increased with the increasing scan rate (Fig. 4a), and a linear relationship between peak current and scan rate in the range from 0.05 to 0.20 V s^{-1} was obtained (Fig. 4b), suggesting that the electrochemical oxidation of NPh at the CTAB-Fe_3O_4-rGO/GCE is a typical adsorption-controlled electrode process. The oxidation peak potential shifted positively with the increase of scan rate (Fig. 4c), with the linear regression equation expressed as E_p (V) = 0.0352 ln$v$ (V s^{-1}) + 0.682 (R^2 = 0.994). For an adsorption-controlled and totally irreversible electrode process, E_p is defined by the Laviron Eq. [31]. Thus, by assuming the charge transfer coefficient (α) to be 0.5, the electron transfer number was calculated to be 1.

The effect of pH value of the buffer on the voltammetric behavior of NPh at the CTAB-Fe_3O_4-rGO/GCE was studied (Fig. 5). The E_p has a negative shift with the increasing of pH value. A linear relationship was obtained between E_p and pH (inset in Fig. 5), and the regression equation is E_p (V) = −0.057 pH + 1.014 (R^2 = 0.985). The slope of the line

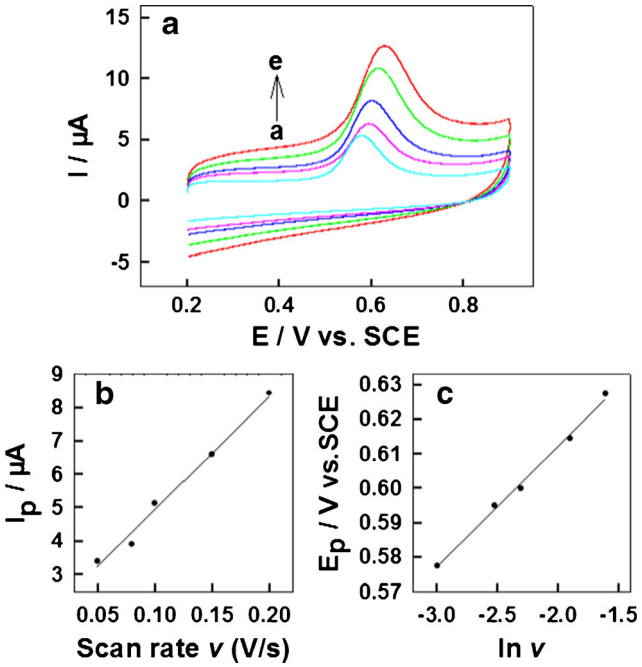

Fig. 4 **a** Cyclic voltammograms of the CTAB-Fe_3O_4-rGO/GCE in 0.1 M phosphate buffer (pH = 7.0) containing 3 μM NPh at different scan rates: (a–e) 0.05, 0.08, 0.10, 0.15, and 0.20 V s^{-1}. **b** The plot of peak current (I_p) vs. scan rate (v). **c** The plot of peak potential (E_p) vs. ln$v$. Accumulation potential: −0.1 V; accumulation time: 300 s

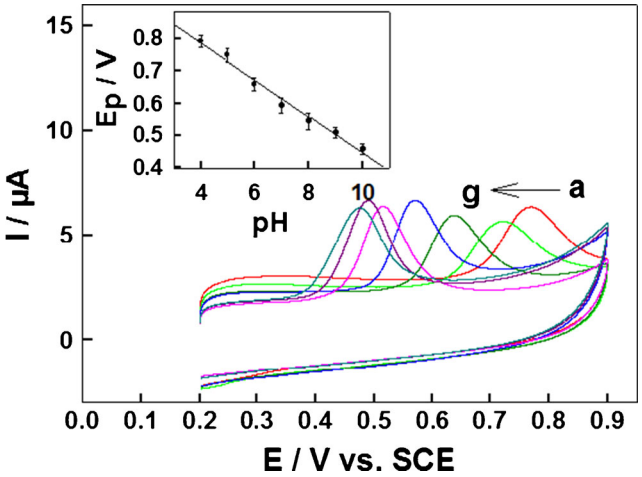

Fig. 5 Cyclic voltammograms of the CTAB-Fe_3O_4-rGO/GCE in 3 μM NPh solutions (phosphate buffer, 0.1 M) with different pH: (a-g) 4.0, 5.0, 6.0, 7.0, 8.0, 9.0 and 10.0. The inset shows the relationship between E_p and pH. Accumulation potential: −0.1 V; accumulation time: 300 s; scan rate: 0.05 V s^{-1}

is −0.057 V pH^{-1}, which is close to the theoretical value −0.059 V pH^{-1}, indicating that an equal number of protons and electrons were involved in the electrochemical oxidation of NPh. The above results have shown that the electron transfer number is 1, thus one proton and one electron attend in the oxidation of NPh at the CTAB-Fe_3O_4-rGO/GCE. According to previous reports on the oxidation of phenolic compounds [32], it is estimated that phenoxy radicals are initially formed as intermediates, which can react irreversibly to form dimeric products.

Optimization of method

The quantitative determination of NPh was performed by DPV, because DPV possesses higher sensitivity and lower detection limit than CV. The following parameters influencing the DPV response current of NPh were optimized: (a) volume of the CTAB-Fe_3O_4-rGO casting solution (1 mg mL^{-1}), (b) accumulation time, (c) accumulation potential. Respective data and figures are given in the Electronic Supplementary Material (Fig. S4 and Fig. S5). We found the following experimental conditions to give the best results: (a) a volume of 4.0 μL of the CTAB-Fe_3O_4-rGO casting solution (1 mg mL^{-1}), (b) an accumulation time of 300 s, (c) an accumulation potential of −0.1 V.

Analytical characteristics

A series of different concentrations of NPh solutions were measured by DPV using the CTAB-Fe_3O_4-rGO/GCE under the optimized conditions, with the results shown in Fig. 6. The peak current gradually enhanced with the increase of NPh concentration. Two linear ranges were obtained from

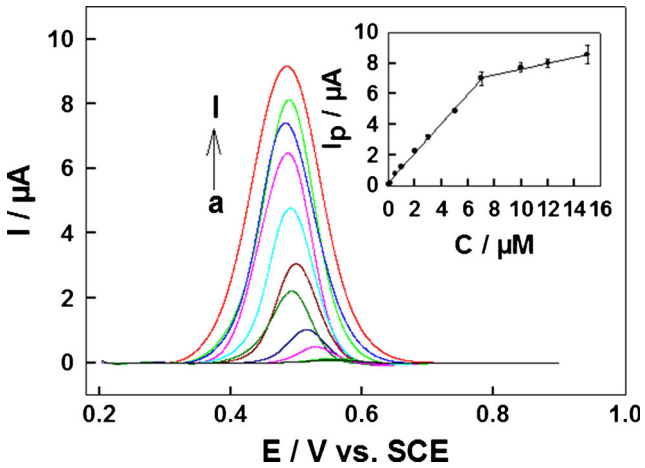

Fig. 6 DPV curves recorded at the CTAB-Fe_3O_4-rGO/GCE in 0.1 M phosphate buffer (pH = 7.0) containing different concentrations of NPh: (a-l) 0.03, 0.05, 0.1, 0.5, 1, 2, 3, 5, 7, 10, 12 and 15 μM. The inset shows the relationship between I_p and NPh concentration. Accumulation potential: −0.1 V; accumulation time: 300 s

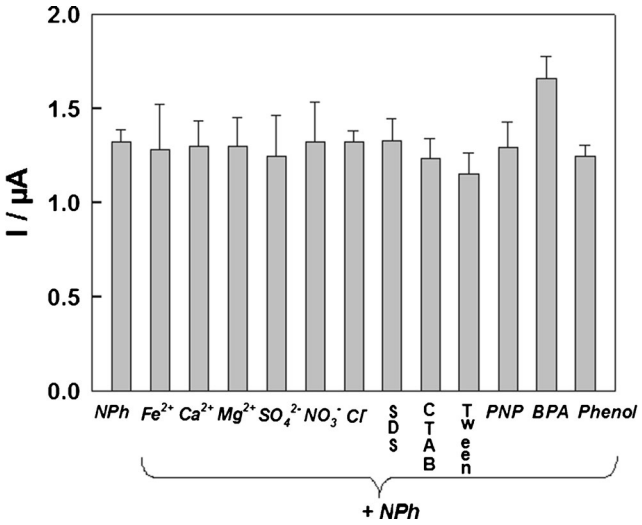

Fig. 7 DPV response currents of the CTAB-Fe_3O_4-rGO/GCE in 0.1 M phosphate buffer (pH = 7.0) containing 1 μM NPh in the absence and presence of 50-fold (50 μM) of Fe^{2+}, Ca^{2+}, Mg^{2+}, SO_4^{2-}, NO_3^-, Cl^-, and 5-fold (5 μM) of SDS, CTAB, Tween-80, *p*-nitrophenol (PNP), bisphenol A (BPA), and phenol, respectively. Accumulation potential: −0.1 V; accumulation time: 300 s

0.03 to 7.0 μM and from 7.0 to 15.0 μM, respectively. The linear regression equations can be expressed as: I_p (μA) = 0.976 C + 0.161 (R^2 = 0.998, C = 0.03–7.0 μM), I_p (μA) = 0.189 C + 5.745 (R^2 = 0.991, C = 7.0–15.0 μM). The detection limit was calculated to be 8 nM (S/N = 3), which is higher than that of LC/MS and HPLC methods [6, 7, 9], but is lower than many previously reported electrochemical methods (Table 1). The sensitivity of our CTAB-Fe_3O_4-rGO/GCE for NPh is 31.1 μA μM^{-1} cm^{-2} in the linear range of 0.03 to 7.0 μM, which is higher than previously reported MIP/sol-gel/MWNTs-Nafion/GCE (1.19 μA μM^{-1} cm^{-2}) [11] and graphene-DNA/GCE (22.0 μA μM^{-1} cm^{-2}) [16].

In order to evaluate the selectivity of the CTAB-Fe_3O_4-rGO/GCE to the detection of NPh, the effects of some possible interfering substances were investigated. From Fig. 7, it can be found that 50-fold of Fe^{2+}, Ca^{2+}, Mg^{2+}, SO_4^{2-}, NO_3^-, Cl^-, and 5-fold of SDS, *p*-nitrophenol (PNP), phenol had no obvious influence on the response of NPh. However, 5-fold of CTAB and Tween-80 resulted in slightly decreased response current probably due to their interactions with NPh. And 5-fold bisphenol A (BPA) resulted in 25% increase of response current. The larger interfering effect of BPA than PNP and phenol was probably due to the hydrophobic groups in BPA, which made BPA more easily adsorb on the nanocomposite.

Table 1 Comparison of the performance of the CTAB-Fe_3O_4-rGO/GCE with previously reported electrodes for the determination of NPh

Electrode	Linear range (μM)	Detection limit (μM)	Reference
MIP/sol-gel/MWNT-NF/GCE	0.2–360	0.06	[11]
GR-DNA/GCE	0.05–4.0	0.01	[16]
β-CD-SH-GR/Au	0.07–70	0.061	[17]
GR-CS/GCE	0.01–40	0.0052	[18]
CTAB/CP electrode	0.1–25	0.01	[27]
Ab/HRP/carbon electrode	0.091–200	0.045	[33]
$FGNS^{IL}$/GCE	0.5–30; 30–200	0.058	[34]
MIPs-TiO_2-AuNPs/Au	0.95–480	0.32	[10]
CTAB-Fe_3O_4-rGO/GCE	0.03–7; 7–15	0.008	This work

The reusability and fabrication reproducibility of the CTAB-Fe_3O_4-rGO/GCE were investigated by measuring the response current to 1 μM NPh. It has been found that the current decreased with the increase of measurements with the same modified electrode, probably due to the accumulation of NPh at the electrode surface. The relative standard deviation (RSD) was 7.7% for the first three measurements, and after five measurements, the electrode retained 72% of its initial sensitivity to NPh. The RSD of the currents for five electrodes, made independently, was 0.9% (Fig. S6), indicating the excellent fabrication reproducibility of the modified electrode.

Analytical application

To further confirm the performance of the CTAB-Fe_3O_4-rGO/GCE in practical analytical application, the NPh contents in Yan Lake water and Pearl River water were determined by DPV. No NPh was found in the two kinds of water samples. The recoveries of 1 μM NPh spiked into the Yan Lake water and the Pearl River water were 102.1% and 99.1%, respectively, illustrating that the CTAB-Fe_3O_4-rGO/GCE was effective and accurate for analyzing NPh in real water samples.

Conclusions

A CTAB-Fe_3O_4-rGO nanocomposite was prepared and used as an electrode material for the electrochemical determination of NPh. The CTAB-Fe_3O_4-rGO modified GCE exhibits a high sensitivity, a low detection limit and a good selectivity for the electrochemical detection of NPh. The reusability of the modified electrode is unsatisfactory probably due to the accumulation of NPh on the electrode surface, but the electrode fabrication procedure is simple and the fabrication reproducibility is good. The CTAB-Fe_3O_4-rGO modified electrode presents a potential application for NPh determination in real water samples.

Acknowledgements This work was financially supported by the National Natural Science Foundation of China (Nos. 51478196, 21575043, 21275056, 21605052, 81371877) and the Special Project of Industry-Academia-Research by Combination of Guangdong Province and Chinese Ministry of Education (2013B090500034).

Compliance with ethical standards The author(s) declare that they have no competing interests.

References

1. Soares A, Guieysse B, Jefferson B, Cartmell E, Lester JN (2008) Nonylphenol in the environment: a critical review on occurrence, fate, toxicity and treatment in wastewaters. Environ Int 34:1033–1049. doi:10.1016/j.envint.2008.01.004
2. Tsuda T, Takino A, Muraki K, Harada H, Kojima M (2001) Evaluation of 4-nonylphenols and 4-tert-octylphenol contamination of fish in rivers by laboratory accumulation and excretion experiments. Wat Res 35:1786–1792
3. Asimakopoulos AG, Thomaidis NS, Koupparis MA (2012) Recent trends in biomonitoring of bisphenol a, 4-t-octylphenol, and 4-nonylphenol. Toxicol Lett 210:141–154. doi:10.1016/j.toxlet.2011.07.032
4. Renner R (1997) European bans on surfactant trigger transatlantic debate. Environ Sci Technol 31:316A–320A
5. Ieda T, Horii Y, Petrick G, Yamashita N, Ochiai N, Kannan K (2005) Analysis of nonylphenol isomers in a technical mixture and in water by comprehensive two-dimensional gas chromatography-mass spectrometry. Environ Sci Technol 39:7202–7207. doi:10.1021/es050568d
6. Loyo-Rosales JE, Schmitz-Afonso I, Rice CP, Torrents A (2003) Analysis of octyl- and nonylphenol and their ethoxylates in water and sediments by liquid chromatography/tandem mass spectrometry. Anal Chem 75:4811–4817. doi:10.1021/ac0262762
7. Asimakopoulos AG, Thomaidis NS (2015) Bisphenol a, 4-t-octylphenol, and 4-nonylphenol determination in serum by hybrid solid phase extraction-precipitation technology technique tailored to liquid chromatography-tandem mass spectrometry. J Chromatogr B 986-987:85–93. doi:10.1016/j.jchromb.2015.02.009
8. Stenholm Å, Holmström S, Hjärthag S, Lind O (2009) Development of a high-performance liquid chromatography-fluorescence detection method for analyzing nonylphenol/dinonylphenol-polyethoxylate-based phosphate esters. J Chromatogr A 1216:6974–6977. doi:10.1016/j.chroma.2009.08.057
9. Zhao R-S, Wang X, Yuan J-P, Zhang L-L (2009) Solid-phase extraction of bisphenol A, nonylphenol and 4-octylphenol from environmental water samples using microporous bamboo charcoal, and their determination by HPLC. Microchim Acta 165:443–447. doi:10.1007/s00604-009-0145-3
10. Huang J, Zhang X, Liu S, Lin Q, He X, Xing X, Lian W, Tang D (2011) Development of molecularly imprinted electrochemical sensor with titanium oxide and gold nanomaterials enhanced technique for determination of 4-nonylphenol. Sensor Actuat B-Chem 152:292–298. doi:10.1016/j.snb.2010.12.022
11. Zhang J, Niu Y, Li S, Luo R, Wang C (2014) A molecularly imprinted electrochemical sensor based on sol-gel technology and multiwalled carbon nanotubes-Nafion functional layer for determination of 2-nonylphenol in environmental samples. Sensor Actuat B-Chem 193:844–850. doi:10.1016/j.snb.2013.11.081
12. Zeravik J, Skryjová K, Nevoranková Z, Fránek M (2004) Development of direct ELISA for the determination of 4-nonylphenol and octylphenol. Anal Chem 76:1021–1027. doi:10.1021/ac030217m
13. Brownson DAC, Banks CE (2010) Graphene electrochemistry: an overview of potential applications. Analyst 135:2768–2778. doi:10.1039/c0an00590h
14. Shao Y, Wang J, Wu H, Liu J, Aksay IA, Lin Y (2010) Graphene based electrochemical sensors and biosensors: a review. Electroanalysis 22:1027–1036. doi:10.1002/elan.200900571
15. Zhu C, Yang G, Li H, Du D, Lin Y (2015) Electrochemical sensors and biosensors based on nanomaterials and nanostructures. Anal Chem 87:230–249. doi:10.1021/ac5039863
16. Zeng L, Zhang A, Zhu X, Zhang C, Liang Y, Nan J (2013) Electrochemical determination of nonylphenol using differential pulse voltammetry based on a graphene-DNA-modified glassy carbon electrode. J Electroanal Chem 703:153–157. doi:10.1016/j.jelechem.2013.05.029
17. Xue F, Gao ZY, Sun XM, Yang ZS, Yi LF, Chen W (2015) Electrochemical determination of environmental hormone nonylphenol based on composite film modified gold electrode. J Electrochem Soc 162:H338–H344. doi:10.1149/2.0271506jes
18. Zhou WS, Zhao B, Huang XH, Yang XD (2013) Electrochemical determination of 4-nonylphenol on graphene-chitosan modified glassy carbon electrode. Chin J Anal Chem 41:675–680. doi:10.1016/S1872-2040(13)60649-0
19. Zhang Y, Cheng Y, Zhou Y, Li B, Gu W, Shi X, Xian Y (2013) Electrochemical sensor for bisphenol A based on magnetic nanoparticles decorated reduced graphene oxide. Talanta 107:211–218. doi:10.1016/j.talanta.2013.01.012
20. Yu L, Wu H, Wu B, Wang Z, Cao H, Fu C, Jia N (2014) Magnetic Fe_3O_4-reduced graphene oxide nanocomposites-based electrochemical biosensing. Nano-Micro Lett 6:258–267. doi:10.5101/nm1140028a
21. Li Y, Zhao X, Li P, Huang Y, Wang J, Zhang J (2015) Highly sensitive Fe_3O_4 nanobeads/graphene-based molecularly imprinted electrochemical sensor for 17β-estradiol in water. Anal Chim Acta 884:106–113. doi:10.1016/j.aca.2015.05.022
22. Li J, Wang X, Duan H, Wang Y, Bu Y, Luo C (2016) Based on magnetic graphene oxide highly sensitive and selective imprinted sensor for determination of sunset yellow. Talanta 147:169–176. doi:10.1016/j.talanta.2015.09.056
23. He Q, Dang X, Hu C, Hu S (2004) The effect of cetyltrimethyl ammonium bromide on the electrochemical determination of thyroxine. Colloids Surf B Biointerfaces 35:93–98. doi:10.1016/j.colsurfb.2004.03.001
24. Hu C, Hu S (2004) Electrochemical characterization of cetyltrimethyl ammonium bromide modified carbon paste electrode and the application in the immobilization of DNA. Electrochim Acta 49:405–412. doi:10.1016/j.electacta.2003.08.022
25. Deng P, Xu Z, Feng Y (2012) Highly sensitive and simultaneous determination of ascorbic acid and rutin at an acetylene black paste electrode coated with cetyltrimethyl ammonium bromide film. J Electroanal Chem 683:47–54. doi:10.1016/j.jelechem.2012.08.002

26. Kor K, Zarei K (2014) Electrochemical determination of chloramphenicol on glassy carbon electrode modified with multi-walled carbon nanotube-cetyltrimethylammonium bromide-poly(diphenylamine). J Electroanal Chem 733:39–46. doi:10.1016/j.jelechem.2014.09.013
27. Lu Q, Zhang W, Wang Z, Yu G, Yuan Y, Zhou Y (2013) A facile electrochemical sensor for nonylphenol determination based on the enhancement effect of cetyltrimethylammonium bromide. Sensors 13:758–768. doi:10.3390/s130100758
28. Xue Y, Chen H, Yu D, Wang S, Yardeni M, Dai Q, Guo M, Liu Y, Lu F, Qu J, Dai L (2011) Oxidizing metal ions with graphene oxide: the *in situ* formation of magnetic nanoparticles on self-reduced graphene sheets for multifunctional applications. Chem Commun 47:11689–11691. doi:10.1039/c1cc14789g
29. Liu M, Wen T, Wu X, Chen C, Hu J, Li J, Wang X (2013) Synthesis of porous Fe_3O_4 hollow microspheres/graphene oxide composite for Cr(VI) removal. Dalton Trans 42:14710–14717. doi:10.1039/c3dt50955a
30. Bard AJ, Faulker LR (2001) Electrochemical methods: fundamentals and applications. John Wiley & Sons, New York
31. Laviron E (1974) Adsorption, autoinhibition and autocatalysis in polarography and in linear potential sweep voltammetry. J Electroanal Chem 52:355–393
32. Ferreira M, Varela H, Torresi RM, Tremiliosi-Filho G (2006) Electrode passivation caused by polymerization of different phenolic compounds. Electrochim Acta 52:434–442. doi:10.1016/j.electacta.2006.05.025
33. Evtugyn GA, Eremin SA, Shaljamova RP, Ismagilova AR, Budnikov HC (2006) Amperometric immunosensor for nonylphenol determination based on peroxidase indicating reaction. Biosens Bioelectron 22:56–62. doi:10.1016/j.bios.2005.11.025
34. Meng X, Yin H, Xu M, Ai S, Zhu J (2012) Electrochemical determination of nonylphenol based on ionic liquid-functionalized graphene nanosheet modified glassy carbon electrode and its interaction with DNA. J Solid State Electrochem 16:2837–2843. doi:10.1007/s10008-012-1710-y